Quantum Electronics **52** (6) 523–527 (2022)

https://doi.org/10.1070/QEL18067

Physical processes during ultracold plasma expansion

B.B. Zelener, S.Ya. Bronin, E.V. Vilshanskaya, E.V. Vikhrov,
K.P. Galstyan, N.V. Morozov, S.A. Saakyan, V.A. Sautenkov, B.V. Zelener

Abstract. **Using the method of molecular dynamics, the expansion of a two-component, pulsed laser-produced ultracold plasma is directly calculated for various values of the number and density of particles and their electron temperatures. A new method is presented for generating and diagnosing a steady-state ultracold plasma formed under continuous wave laser irradiation. The performed calculations show the difference in the properties of an ultracold plasma obtained by pulsed and continuous wave laser irradiation.**

Keywords: *magneto-optical trap, ultracold plasma, molecular dynamics method.*

1. Introduction

The creation of a magneto-optical trap (MOT) in 1987 [1] led to the emergence of new unique scientific directions, which resulted in the obtaining of Bose–Einstein condensation [2] and a degenerate Fermi gas [3], as well as in the development of ultra-precise atomic clocks [4] and quantum gravimeters [5]. Based on cold alkali metal atoms, Beterov et al. [6] implemented qubits for problems of quantum informatics. Ultracold plasma (UCP) was first obtained by Killian et al. [7] from xenon atoms cooled in an MOT. An interesting development of UCP experiments was the use of alkaline earth metal atoms [8], which made it possible to observe the fluorescence of ions in the optical range.

B.B. Zelener Joint Institute for High Temperatures, Russian Academy of Sciences, ul. Izhorskaya 13, stroenie 2, 125412 Moscow, Russia; National Research Nuclear University MEPhI, Kashirskoe sh. 31, 115409 Moscow, Russia; National Research University MPEI, ul. Krasnokazarmennaya 14, 111250 Moscow, Russia;
e-mail: bobozel@mail.ru;
S.Ya. Bronin, E.V. Vilshanskaya, B.V. Zelener Joint Institute for High Temperatures, Russian Academy of Sciences, ul. Izhorskaya 13, stroenie 2, 125412 Moscow, Russia;
E.V. Vikhrov, K.P. Galstyan, N.V. Morozov Joint Institute for High Temperatures, Russian Academy of Sciences, ul. Izhorskaya 13, stroenie 2, 125412 Moscow, Russia; National Research Nuclear University MEPhI, Kashirskoe sh. 31, 115409 Moscow, Russia;
S.A. Saakyan Joint Institute for High Temperatures, Russian Academy of Sciences, ul. Izhorskaya 13, stroenie 2, 125412 Moscow, Russia; National Research University – Higher School of Economics, Pokrovsky blvd. 11, 109028 Moscow, Russia;
V.A. Sautenkov Joint Institute for High Temperatures, Russian Academy of Sciences, ul. Izhorskaya 13, stroenie 2, 125412 Moscow, Russia; P.N. Lebedev Physical Institute of the Russian Academy of Sciences, Leninsky prosp. 53, 119991 Moscow, Russia

3 March 2022; revision received 15 April 2022
Kvantovaya Elektronika **52** (6) 523–527 (2022)
Translated by I.A. Ulitkin

In UCP experiments, the density of charged particles varies from 10^3 to 10^{11} cm^{-3}. The plasma is sufficiently rarefied, and so the interaction of charged particles with neutral atoms can be neglected in comparison with the Coulomb interaction. In addition, the density of charged particles imposes restrictions on the minimum temperature of the plasma and, consequently, on strongly coupled parameter of the plasma, which is defined as the ratio of the average potential energy to the kinetic energy of the particles. As was shown by Bergeson et al. [9], in times much shorter than the plasma expansion time, due to the conversion of the potential Coulomb energy into kinetic energy, the plasma experiences rapid disorder-induced heating (DIH) up to a temperature

$$T_{\mathrm{DIH}} \approx \frac{e^2}{9.2\pi a \varepsilon_0 k}, \tag{1}$$

where e is the electron charge; k is the Boltzmann constant; a is the radius of the Wigner–Seitz cell; and ε_0 is the electric constant. As a result, the minimum temperature of plasma ions increases from 0.05 K at a density of 10^5 cm^{-3} to 5 K at a density of 10^{11} cm^{-3}. The maximum strongly coupled parameter for ions, regardless of their concentration, is 2.3.

The initial kinetic energy of electrons in the experiment is easily controlled and is determined by the frequency detuning of the ionising laser radiation from the ionisation potential in the range from 0 to 200 K. The minimum initial kinetic energy of electrons is chosen such that no more than 1% of electrons are recombined in the UCP.

There is no degeneracy in the UCP, and its properties can be calculated by classical methods, including the molecular dynamics method (MDM). It was shown in Refs [10–15] that the properties of such a plasma expressed in a dimensionless form – charge diffusion coefficients, conductivity, thermal conductivity, viscosity, permittivity, and refraction, absorption and reflection coefficients, as well as the probability of ionic microfield distribution – correspond to any classical strongly coupled nondegenerate plasma with different degrees of ionisation.

The study of UCP expansion into vacuum is of particular interest. In contrast to a high-temperature plasma, the UCP is characterised by a slow expansion velocity and a large strongly coupled parameter. An experiment with well-controlled initial conditions makes it possible to study in detail the dynamics of plasma expansion and the effect on the strongly coupled parameter on it. Initially, the UCP of various elements (Xe, Sr, Rb, and Ca) was obtained by single ionisation of an ultracold gas in a MOT in a high vacuum using a pulsed laser [7, 16, 17]. The advantage of these experiments lies in the possibility of producing and studying a strongly coupled, high-density UCP.

One of the best ways to study the UCP expansion process with maximum accuracy and thoroughness is to simulate it by the molecular dynamics method. However, the implementation of this method for the experimentally used number of particles, $N = 10^6 - 10^8$, interacting according to the Coulomb law, encounters a huge amount of required calculations, and therefore only calculations for a quasi-electrically neutral plasma have been performed so far using the hydrodynamic approximation, which distort the real description of the occurring processes. In our calculations, we simulated the expansion of the UCP using MDM with electrons and ions of real mass. Based on the calculations made for $N = 10^3 - 10^5$, we were able to determine the general regularities in the process of expansion of a plasma cloud formed by a pulsed laser. The resulting approximations made it possible to establish the main characteristics of the expansion for the real number of particles in the experiment up to $N \approx 10^8$ [18, 19].

A significant drawback of the UCP produced by pulsed laser radiation is its lifetime limited to microseconds, which sufficiently complicates the experiments. In addition, an increase in the UCP density leads to an increase in temperature due to the rapid heating of the plasma and to a further decrease in the time of its expansion.

Previously, in paper [20] we proposed a method for generating and studying UCP using cw lasers. In this case, the atoms that constantly enter and cool into the MOT are continuously ionised. The charge particles are not held in the MOT and leave it over time. However, as a result of continuous ionisation, at a certain point in time, which depends on the initial energy of electrons and ions, as well as on the plasma density, a steady-state distribution of plasma particles in density and temperature is quickly established, which can exist for a long time.

The formation of a steady-state UCP when it was produced by a cw laser was calculated using MDM [21]. As in the case of the expansion of plasma particles generated by a pulsed laser, a charge imbalance is also formed in the steady-state regime, which produces an electric field that confines electrons and accelerates ions. The behaviour of the field strength in the plasma cloud in this case corresponds to the behaviour of that for a uniformly charged ball. A steady-state distribution of plasma particles is obtained as a function of the parameters, and the difference between the expansion of particles in a steady-state plasma and the expansion in the case of a pulsed method of its generation is shown.

In the present work, we report a detailed analysis of the physical processes during the expansion of the UCP. Section 3 presents the results of a direct calculation of the expansion of a two-component UCP obtained with a pulsed laser for various values of the number of particles, densities, and electron temperatures. The self-similar character of the plasma expansion process is demonstrated. Section 4 describes a new method for producing and diagnosing a steady-state UCP by a cw laser. Section 5 presents numerical calculations by the method of molecular dynamics, which show the difference between the properties of the UCPs obtained with pulsed and continuous wave laser irradiation.

2. Physical model and calculation method

We consider a system of particles consisting of singly charged ions and electrons; at the initial moment of time, the concentrations of electrons and ions are equal: $n_{e0} = n_{i0}$. The interaction of particles is described by the Coulomb law. To avoid computational difficulties for interacting particles, the potential function is modified:

$$U(r_{jk}) = -\frac{e^2}{r_{jk} + r_0}, \quad j \neq k, \tag{2}$$

where j and k define the particle type;

$$r_0 = \alpha n^{-1/3} \tag{3}$$

is some minimum distance at which the particles can approach each other, expressed in terms of the average distance between the particles; n is the concentration of particles; and $\alpha \sim 0.03$. The value of r_0 is rather small and does not affect the accuracy of calculations.

At a zero moment of time, the velocities of both types of particles have a Maxwellian distribution at a given temperature. The initial coordinates are set such that the particle density obeys the normal distribution law, the dispersion of which depends on the concentration. To integrate the equations of motion, use is made of the Verlet scheme in the velocity form. The minimum time step in calculating the motion of electrons is $\tau_e = 10^{-12}$ s. Because the particle masses differ significantly, the time step is chosen for ions and electrons to be different (proportional to the square root of the mass ratio). This technique allows one to speed up calculations without decreasing accuracy. To reduce the computation time, we use an algorithm for parallelising calculations specially developed by us for our program. In the process of calculations, energy conservation was ensured with an accuracy of 1%.

3. Calculation of the expansion of a pulsed laser-produced plasma

The initial spatial distribution of electrons and ions is assumed to be Gaussian:

$$n_{i,e}(\boldsymbol{r}) = n \exp\left(-\frac{r^2}{2\sigma_0^2}\right), \tag{4}$$

where $\sigma_0 = (N/n)^{1/3}/(2\pi)^{1/2}$ is the initial plasma size, and $N = N_e = N_i$ is the initial number of particles.

The expansion of the plasma begins when the fastest electrons leave it; as a result, an electric charge $Q = e\Delta N_e$ is formed in the main plasma region, where ΔN_e is the number of electrons that have left the main plasma region. The characteristic time of this process is $t \sim \sigma_0/v_{T_e} = \sigma_0\sqrt{m_e/(kT_{e0})} \sim 10^{-7} - 10^{-8}$ s, where kT_{e0} and m_e are the initial kinetic energy and electron mass. The electrons remaining in the plasma are held in it by the formed potential barrier. At the beginning of the expansion, the energy of the electrons is converted into the energy of the electric field, which then, accelerating the ions, transfers energy to the ion component. At the final stage of plasma expansion, the energy of the electric field tends to zero, and the energy exchange between the two plasma components stops.

The MDM calculations make it possible to obtain the values of ΔN_e for finite, not too large values of the number of particles, $N \sim 10^5$. To estimate the parametric dependence for large N, use is made of the system of equations described in [18], which are characteristics of the Boltzmann equation for the electronic component at times that are sufficiently small, so that the displacement of the ions can be neglected.

The natural dimensionless parameters on which the expansion parameters can depend are the number of particles N and the parameter N^* introduced in [7]:

$$N^* = \frac{3}{2}\sqrt{\frac{\pi}{2}}\frac{kT_{e0}\sigma_0}{e^2}. \quad (5)$$

The characteristic scale of the charge is determined by the energy scale of the system, $W \sim kT_{e0}N_e$:

$$\frac{Q^2}{\sigma_0} = \frac{e^2\Delta N_e^2}{\sigma_0} \sim kT_{e0}N, \quad (6)$$

$$\Delta N_e \sim \frac{1}{e}\sqrt{kT_{e0}N_e\sigma_0} \sim \sqrt{NN^*}. \quad (7)$$

The experimental results reported in [7] indeed point to a simple approximate relationship between $\Delta N_e/N$ and N^*/N. Figure 1 shows the fraction of electrons remaining in the plasma, $1 - \Delta N_e/N$, as a function of the parameter N^*/N, obtained in the experiment [7] and in our calculations, for different initial electron temperatures. The initial plasma size is $\sigma_0 = 0.02$ cm.

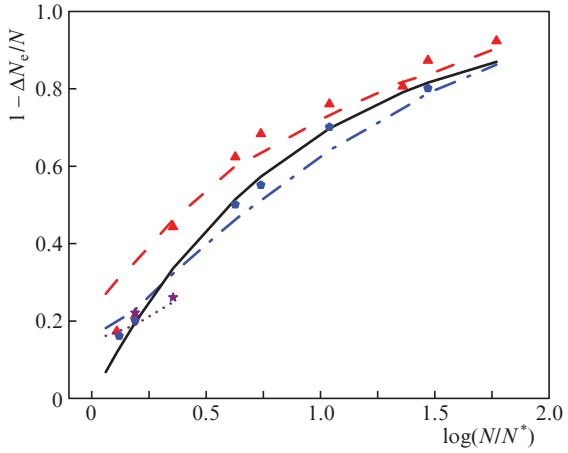

Figure 1. (Colour online) Dependences of the fraction of electrons remaining in the plasma $1 - \Delta N_e/N$ on the parameter N/N^* obtained by calculation (curves) and experimentally [7] (dots) at initial electron temperatures $T_{e0} = 3.9$ K (red dashed line and triangles), $T_{e0} = 34.5$ K (blue dash-dotted line and pentagons) and $T_{e0} = 314$ K (purple dotted line and asterisks), as well as dependence $1 - \Delta N_e/N \approx 1 - (N^*/N)^{1/2}$ (solid black curve).

The excess positive charge remaining in the plasma is localised in a narrow layer at its outer boundary at $r > 2\sigma(t)$, where $\sigma^2(t) = \langle r^2\rangle/3$. Its formation characteristic time t is determined by the ion velocity and plasma size: $t \sim \sigma_0 \times 1/\sqrt{kT_{e0}/m_i}$. Under typical experimental conditions and for the calculation parameters given here, the time t is ~1 μs. According to numerical calculations, this layer has a characteristic front shape with a sharp drop in charge concentration.

As the plasma expands, the rate of displacement of the charged layer V_Q, as well as the rate V_σ of the change in plasma size $\sigma(t)$, become constant with the ratio between them remaining at a level of 2.5.

The radial dependence of the electric field has a pronounced maximum in the region of the charged layer. Let us define the dimensionless strength $\mathcal{E}$ of the electric field strength $E(r,t)$ as

$$E(r,t) \approx \frac{e\Delta N_e}{\sigma^2(t)}\mathcal{E}(\xi), \quad \xi = \frac{r}{\sigma(t)}. \quad (8)$$

The dimensionless function $\mathcal{E}(\xi)$ of the dimensionless quantity ξ is approximately the same for all values of the plasma parameters at times when the positive charge layer has been formed. In a wide range of plasma parameters N, n, and T_{e0}, as well as at $t > 10$ μs, the function $\mathcal{E}(\xi)$ is virtually unchanged (its values differ by no more than 5%) and has a characteristic maximum near $\xi \approx 2.5$. Figure 2 shows the average value of $\mathcal{E}(\xi)$, which takes into account the dependence on the number of particles, density, temperature, and expansion time.

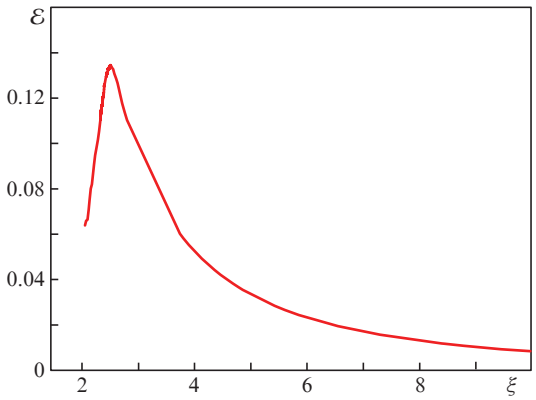

Figure 2. (Colour online) Dimensionless averaged value $\mathcal{E}(\xi)$ (8), taking into account the dependence on the number of particles, their density, temperature, and time of expansion.

At the final stage of the plasma expansion, the electric field amplitude decreases as $\sim 1/t^2$, but the strength of the weakening field is sufficient to keep the remaining electrons in the plasma region during the entire expansion process. These electrons account for no more than 5% of the kinetic energy in this region, which is determined by the kinetic energy of the ions. In this case, the thermal energy of ions is always negligibly small compared to the energy of their radial motion.

Thus, the molecular dynamics simulation shows that under all the considered conditions, the nature of the expansion process is the same. After the escape of fast electrons from the plasma cloud, the excess positive charge is localised at the outer boundary in a narrow layer, which has a characteristic front shape with a sharp decrease in the charge concentration. As the plasma expands, the velocity of the charged layer becomes constant and significantly exceeds the sound velocity of the ions. In this case, the dependence of the radial velocity of ions on the radius acquires a self-similar character long before the final stage of expansion.

4. Experiment on the UCP generation in a steadu-state regime

To produce a UCP in a steady-state regime, we initially created a MOT of ^{40}Ca atoms, which operates on transitions corresponding to wavelengths of 423 nm (main cooling transi-

tion) and 672 nm (optical pumping) [22, 23]. Plasma is generated from cooled calcium atoms trapped in the MOT using cw ionising laser radiation with a wavelength λ = 390 nm (with a detuning above the ionisation threshold). The calcium ion has strong transitions in the optical range, which are used for laser-induced fluorescence (LIF) of ions. The energy level diagrams of the ^{40}Ca atom and ion are shown in Fig. 3.

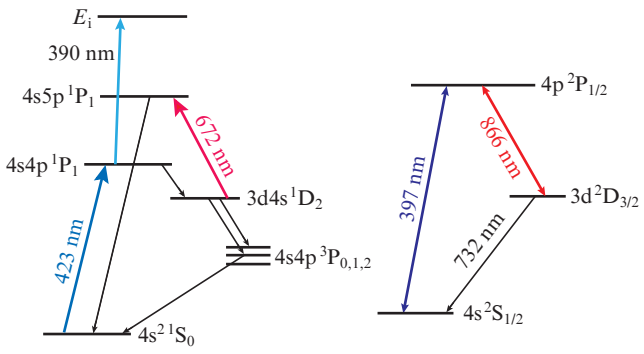

Figure 3. (Colour online) Energy level diagrams of the ^{40}Ca atom and $^{40}Ca^+$ ion.

In the experiment, the fluorescence of ^{40}Ca ions is recorded by a CCD camera using an interference filter and a photomultiplier tube (PMT) with a diffraction grating (Fig. 4). Fluorescence of ^{40}Ca ions was obtained using laser radiation at λ = 397 nm with an intensity of 1.5×10^4 W m^{-2} and with constant optical pumping by a laser at λ = 866 nm with an intensity of 0.4×10^4 W m^{-2} (the radii of both beams are about 10^{-3} m).

Using stationary kinetic equations, we determined the concentration of ions in the generated UCP:

$$n_i = \frac{\eta n_a \tau_i}{\tau_{MOT}}, \quad (9)$$

where n_a is the peak concentration of neutral atoms, which was determined by absorption imaging (typical value 3×10^9 cm^{-3}); η is the fraction of ionised atoms (determined by the drop in the fluorescence signal of neutral atoms in the MOT when the ionising laser is turned on at λ = 390 nm); τ_{MOT} is the lifetime of neutral atoms in the MOT after the cessation of the influx of new atoms (typical value 0.2 s); and τ_i is the expansion time of UCP ions, which is determined by the dynamics of the ion fluorescence signal drop when the ionising laser is turned off at λ = 390 nm (the characteristic expansion time is 3×10^{-5} s). Despite the low concentration of ions (up to 10^6 cm^{-3} at a temperature of ~0.1 K), the UCP strongly interacts with an ion strongly coupled parameter of about unity.

5. Calculation of a stady-state plasma

When a plasma is produced by a cw laser in a stedy-state regime (as in the case of its expansion), a charge imbalance is also created, which forms an electric field that confines electrons and accelerates ions. In this case, the field strength in the plasma cloud corresponds to the behaviour of the field strength of a uniformly charged ball. With the help of MDM, we obtained a steady-state distribution of plasma particles as a function of the parameters and demonstrated the difference between the expansion of particles in a steady-state plasma and the expansion due to the pulsed method of its creation.

To simulate the formation of a steady-state UCP by MDM, we used the physical model presented in Section 2, taking into account the constant production of new plasma particles. In this case, in the region of ~0.1 cm, two pairs of pairs of charged particles (an electron and a ^{40}Ca ion) appeared every 10^{-7} s. Their coordinates had a Gaussian distribution with a dispersion of ~0.1 cm, and their velocities had a Maxwellian distribution with a given initial kinetic energy. When solving the equations of motion, the Coulomb interaction between particles (all particles with all) was taken into account. All these conditions were chosen based on the analysis of experimental data.

The experiments used a magnetic field with a strength of about 30 G cm^{-1}. The average field acting on the plasma is about 1 G in a region with a radius of 0.5 mm. A charged particle is held in a magnetic trap if its Larmor radius is small compared to the size of the trap across the magnetic field. The calculation was performed for an initial electron energy of 5 K. At this energy, the Larmor radius of an electron is 0.9 mm, while for ions it is much larger. This estimate shows that the influence of the magnetic field on the plasma expansion dynamics can be neglected.

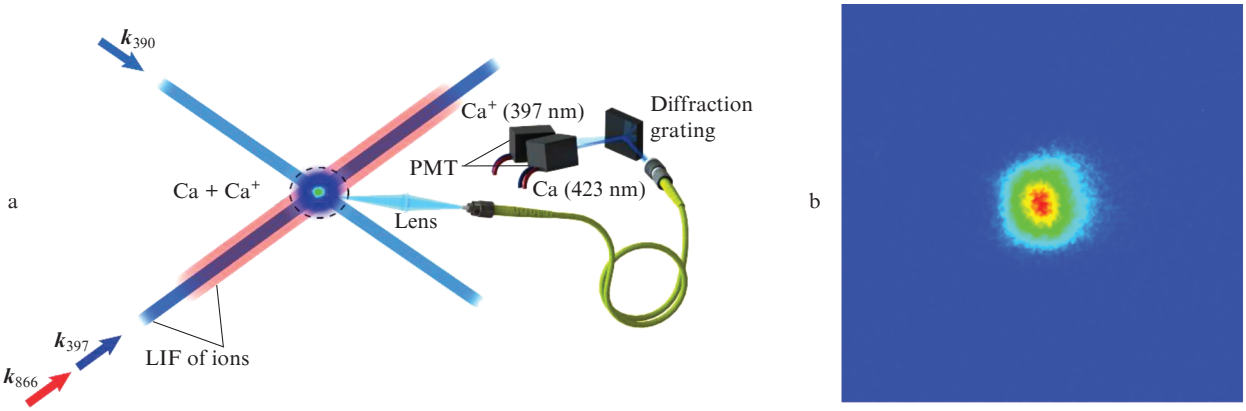

Figure 4. (Colour online) (a) Scheme of the setup for obtaining a steady-state UCP from ^{40}Ca and (b) photograph of the fluorescence of ions of a steady-state UCP from $^{40}Ca^+$ at a wavelength of 397 nm, with the colour corresponding to the fluorescence intensity gradient.

Figure 5a shows the ion density distributions as functions of the radius of the plasma cloud for different times t at initial electron and ion temperatures $T_{e0} = 5$ K and $T_{i0} = 10^{-3}$ K, respectively. One can seen that the steady-state regime is established at $t \approx 200$ μs. The density of ions in the centre under given initial conditions reaches 1.2×10^5 cm^{-3}, which approximately corresponds to experimental estimates.

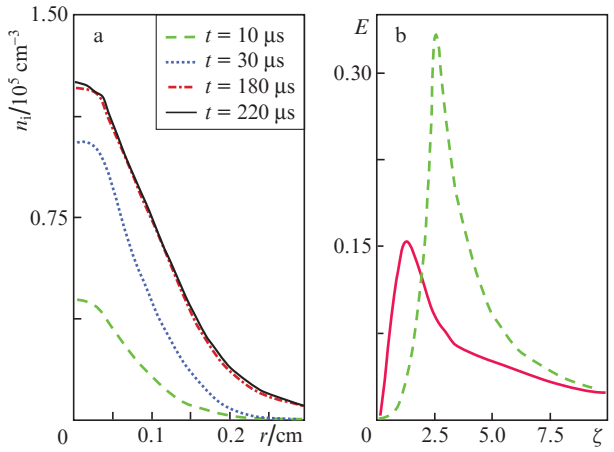

Figure 5. (Colour online) (a) Dependences of the ion concentration on the radius for different moments of time t at $\sigma = 0.07$ cm and (b) dimensionless distributions of the electric field E in the steady-state regime at $\sigma = 0.07$ cm and $t = 200$ μs (solid red curve) and in the pulsed regime (green dashed curve).

One of the important differences between the formation of a steady-state plasma and the case of its formation with the help of a pulsed laser is the difference in the behaviour of the electric field. Figure 5b shows the dimensionless distributions of the electric field E as a function of $\zeta = r/\sigma_r$, where $\sigma_r = \sqrt{\langle r^2 \rangle}$, for a steady-state regime and pulsed ionisation. The field values are normalised so that $\int E(\zeta)d\zeta = 1$. The observed difference in the behaviour of the electric field is due to the fact that in the pulsed version, the excess charge is concentrated in a narrow layer at the plasma edge, while in the steady-state case, the charge in the plasma region is uniformly distributed.

6. Conclusions

The paper presents a universal method for direct calculation of the expansion of a two-component UCP, which allows one to determine the dynamics and nature of the expansion of electrons and plasma ions. The similarity of the nature of the UCP expansion with different numbers of particles, density, temperature, and expansion time is demostrated. A good agreement between the calculations and the available experimental data is obtained. A new method for producing and diagnosing a steady-state UCP using cw lasers is also described. Molecular dynamics simulation of the formation of a steady-state UCP with a constant source of new ions and electrons shows a fairly fast establishment of a steady-state distribution of plasma particles in density and temperature, which can exist for a long time and have a strongly coupled parameter of about unity. The results obtained give grounds to use this method of calculation, as well as UCP experiments, to predict the dynamics and character of plasma expansion with a higher temperature and concentration. In the future, we intend to investigate the UCP properties in magnetic and alternating electric fields.

Acknowledgements. The work was supported by the Russian Science Foundation (Grant No. 18-12-00424) and also by the Ministry of Science and Higher Education of the Russian Federation (State Task No. 075-01056-22-00) in part of the development of a program using parallel computing algorithms for performing calculations at the Joint Supercomputing Centre of the Russian Academy of Sciences.

References

1. Phillips W.D. *Rev. Mod. Phys*., **70**, 721 (1998).
2. Il'ichov L.V., Chapovsky P.L. *Quantum Electron*., **47**, 463 (2017) [*Kvantovaya Elektron*., **47**, 463 (2017)].
3. Makhalov V.B., Turlapov A.V. *Quantum Electron*., **48**, 401 (2018) [*Kvantovaya Elektron*., **48**, 401 (2018)].
4. Fedorova E.S., Tregubov D.O., Golovizin A.A., Mishin D.A., Provorchenko D.I., Khabarova K.Yu., Sorokin V.N., Kolachevsky N.N. *Quantum Electron*., **50**, 220 (2020) [*Kvantovaya Elektron*., **50**, 220 (2020)].
5. Afanasiev A.E., Kalmykov A.S., Kirtaev R.V., Kortel A.A., Skakunenko P.I., Negrov D.V., Balykin V.I. *Opt. Laser Technol*., **148**, 107698 (2022).
6. Beterov I.I., Yakshina E.A., Tretyakov D.B., Entin V.M., Al'yanova N.V., Mityanin K.Yu., Faruk A.M., Ryabtsev I.I. *Quantum Electron*., **51**, 464 (2021) [*Kvantovaya Elektron*., **51**, 464 (2021)].
7. Killian T.C., Kulin S., Bergeson S.D., Orozco L.A., Orzel C., Rolston S.L. *Phys. Rev. Lett*., **83**, 4776 (1999).
8. McQuillen P., Zhang X., Strickler T., Dunning F.B., Killian T.C. *Phys. Rev. A*, **87**, 013407 (2013).
9. Bergeson S.D., Baalrud S.D., Ellison C.L., Grant E., Graziani F.R., Killian T.C., Murilo M.S., Roberts J.L., Stanton L.G. *Phys. Plasmas*, **26**, 100501 (2019).
10. Bobrov A.A., Bunkov A.M., Bronin S.Y., Klyarfeld A.B., Zelener B.B., Zelener B.V. *Phys. Plasmas*, **26**, 082102 (2019).
11. Bobrov A.A., Bronin S.Y., Klyarfeld A.B., Zelener B.B., Zelener B.V. *Phys. Plasmas*, **27**, 010701 (2020).
12. Bobrov A.A., Bronin S.Y., Korchagin D.S., Zelener B.B., Zelener B.V. *Phys. Plasmas*, **27**, 122103 (2020).
13. Bronin S.Y., Korchagin D.S., Zelener B.B., Zelener B.V. *Phys. Plasmas*, **28**, 112106 (2021).
14. Bronin S.Y., Zelener B.B., Zelener B.V. *J. Quant. Spectrosc. Radiat. Transf*., **268**, 107621 (2021).
15. Bronin S.Y., Zelener B.B., Zelener B.V. *Plasma Sources Sci. Technol*., **30**, 115018 (2021).
16. Killian T.C., Pattard T., Pohl T., Rost J.M. *Phys. Rep*., **449**, 77 (2007).
17. Lyon M., Rolston S.L. *Rep. Porg. Phys*., **80**, 017001 (2017).
18. Vikhrov E.V., Bronin S.Y., Klayrfeld A.B., Zelener B.B., Zelener B.V. *Phys. Plasmas*, **27**, 120702 (2020).
19. Vikhrov E.V., Bronin S.Y., Zelener B.B., Zelener B.V. *Phys. Rev. E*, **104**, 015212 (2021).
20. Zelener B.B., Vilshanskaya E.V., Saakyan S.A., Sautenkov V.A., Zelener B.V., Fortov V.E. *JETP Lett*., **113**, 82 (2021) [*Pis'ma Zh. Eskp. Teor. Fiz*., **113**, 92 (2021)].
21. Bronin S.Ya., Vikhrov E.V., Zelener B.B., Zelener B.V. *JETP Lett.*, **114**, 572 (2021) [*Pis'ma Zh. Eskp. Teor. Fiz*., **114**, 643 (2021)].
22. Vilshanskaya E.V., Saakyan S.A., Sautenkov V.A., Zelener B.B. *J. Phys. Conf. Ser*., **1147**, 012097 (2019).
23. Zelener B.B., Arshinova I.D., Bobrov A.A., Vilshanskaya E.V., Sahakyan S.A., Sautenkov V.A., Zelener B.V., Fortov V.E. *JETP Lett*., **108**, 820 (2018) [*Pis'ma Zh. Eskp. Teor. Fiz*., **108**, 829 (2018)].